Supporting Information

Kinetics-Driven Crystal-Facets Evolution at the Tip of Nanowires – A New Implementation of the Ostwald-Lussac Law

Xin Yin,[1] Xudong Wang[1,*]

1. Department of Materials Science and Engineering, University of Wisconsin-Madison, Madison, WI 53706

*Email: xudong.wang@wisc.edu

S1 Experiment section

S1.1 Synthesis process

5 g zinc oxide powder was weighed as the precursor and loaded in an alumina boat. The boat was then placed at the center of an alumina tube located inside a single-zone tube furnace. Argon carrier gas with the flow rate of 50 sccm and oxygen carrier gas with the flow rate of 5 sccm were applied and the pressure inside the tube was kept at 53 Pa. Three polycrystalline alumina substrates (11.4 cm in length and 1 cm in width) were lined together in the tube which covered a broad deposition temperature. The system temperature reached 1273 K during the first 40 minutes and reached 1673 K after another 50 minutes. The precursor completely decomposed and vaporized before the temperature reached 1673 K. Subsequently, the system was cooled down to room temperature naturally under the same argon atmosphere.

S1.2. Electronic microscopy characterization

Zeiss LEO 1530 Schottky-type field-emission scanning electron microscope was used to study the morphologies of the samples. X–ray diffraction was acquired from Bruker D8 Discovery with Cu Kα radiation. FEI TF30 transmission electron microscope operated at 300 kV was used to study the crystal structure of the samples.

S2. Large scale of ZnO NWs grown on polycrystalline alumina substrate.

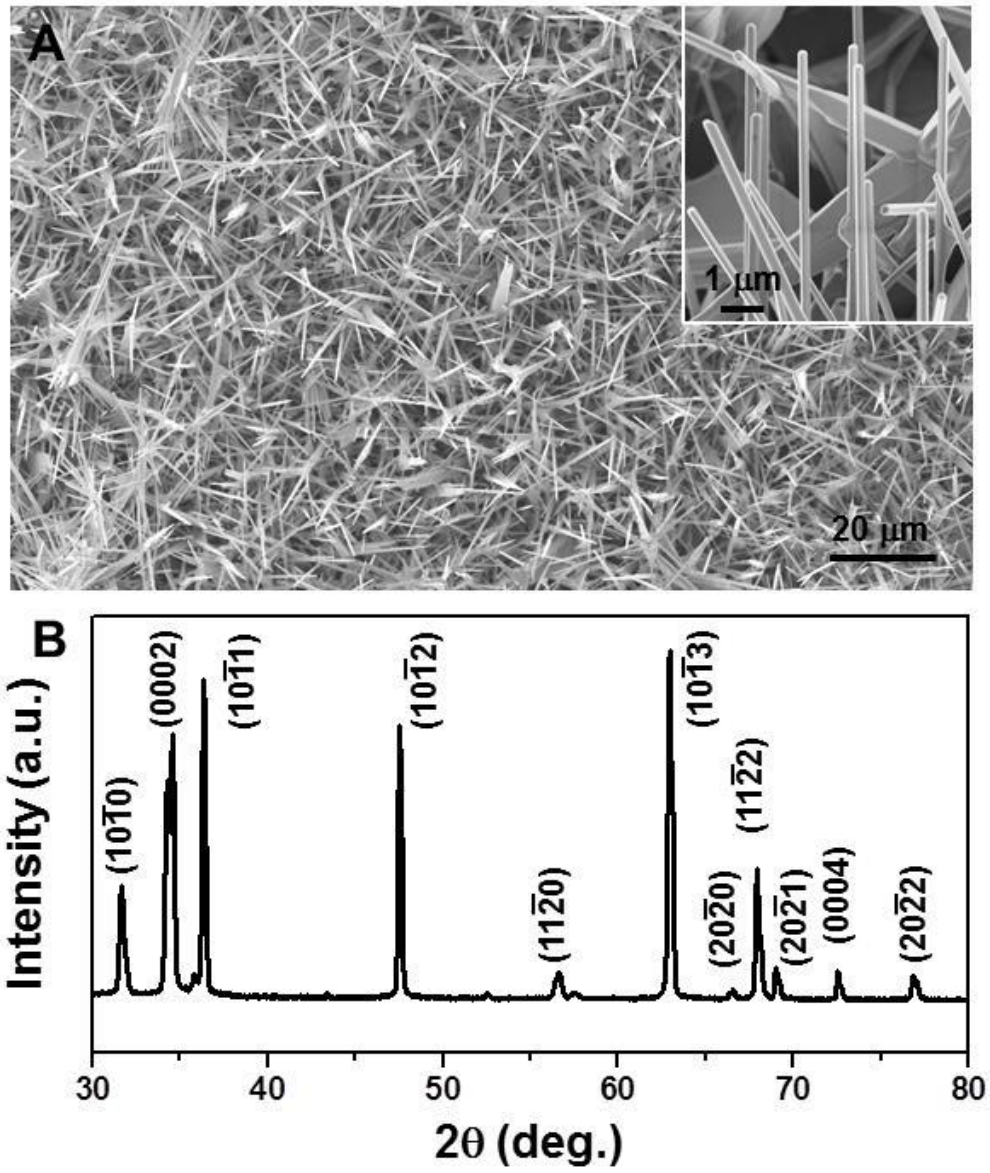

Figure S1. (A) SEM image of ZnO NWs in a large area, inset: the enlarged SEM image of a few individual NWs with faceted tip. (B) X-ray diffraction pattern of ZnO nanorods.

S3. Relationship between deposition temperature and deposition location in the reaction chamber.

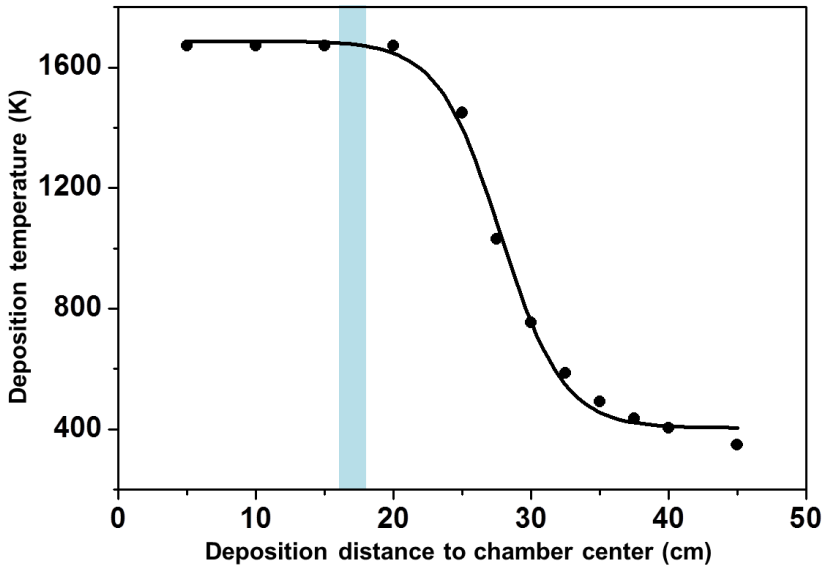

Figure S2. Deposition temperature along the reaction chamber. The facet evolution region is highlighted in blue.

S4. Tip facet evolutions at large scale.

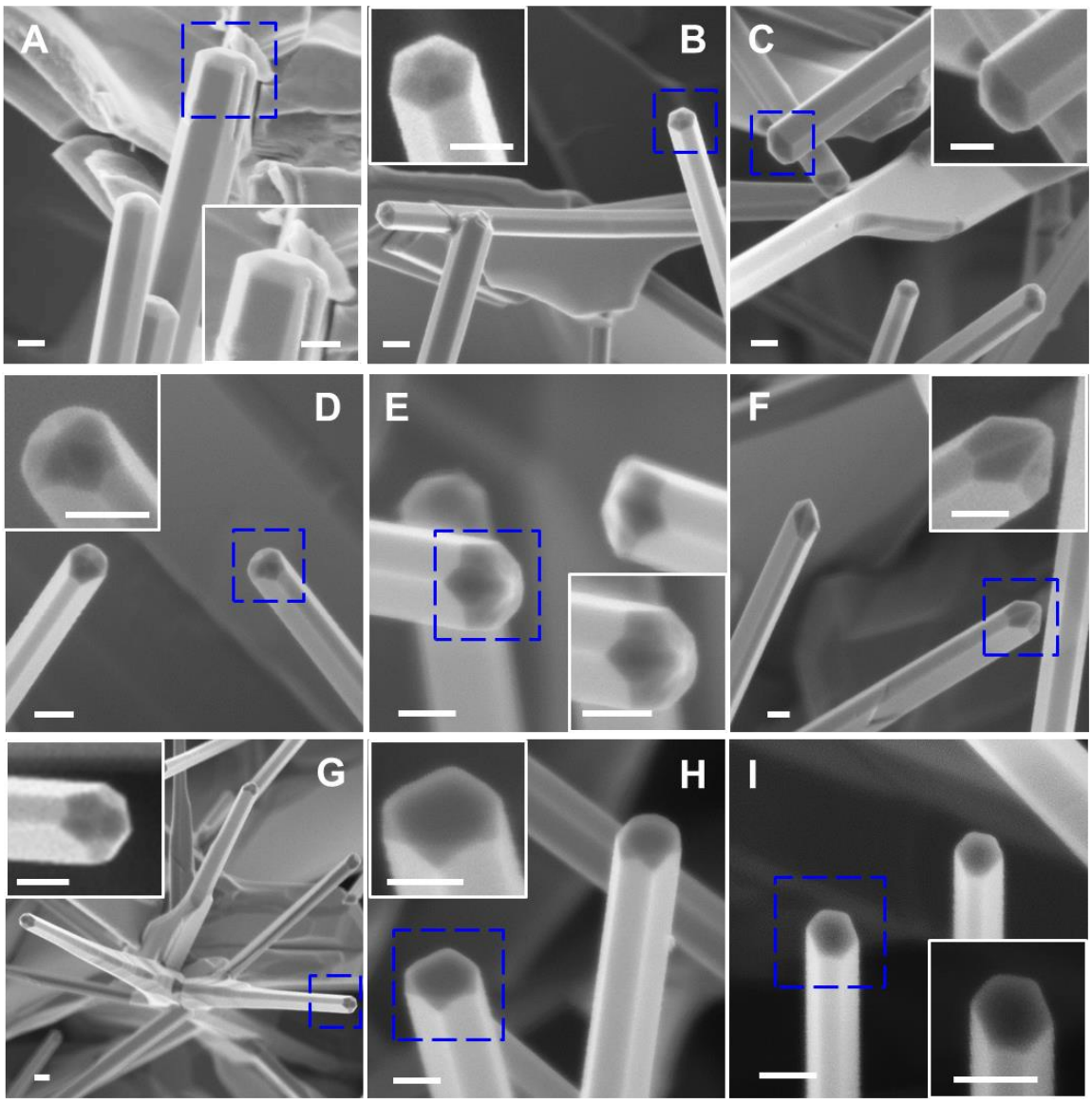

Figure S3. Large scale SEM images of the facet evolution, corresponding to each image of Figure 1 in the main text. Each facet combination exhibits good uniformity within a finite small area where the deposition conditions are nearly identical. The inset is the enlarged image of thetip in the dashed blue box. The scale bars are 200 nm.

S5. Statistical data of the growth rate ratio depending on the locations.

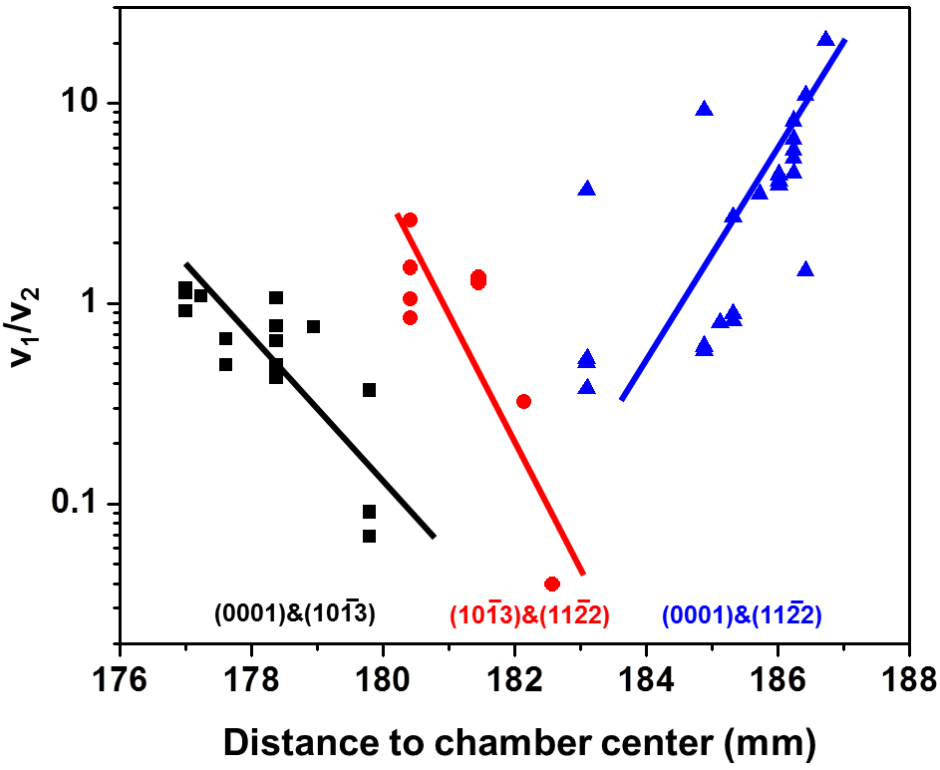

Figure S4. Relationship between the growth rate ratio and the deposition locations, showing the facet evolution trend.

S6. Atomic structures of the facets involved in the growth

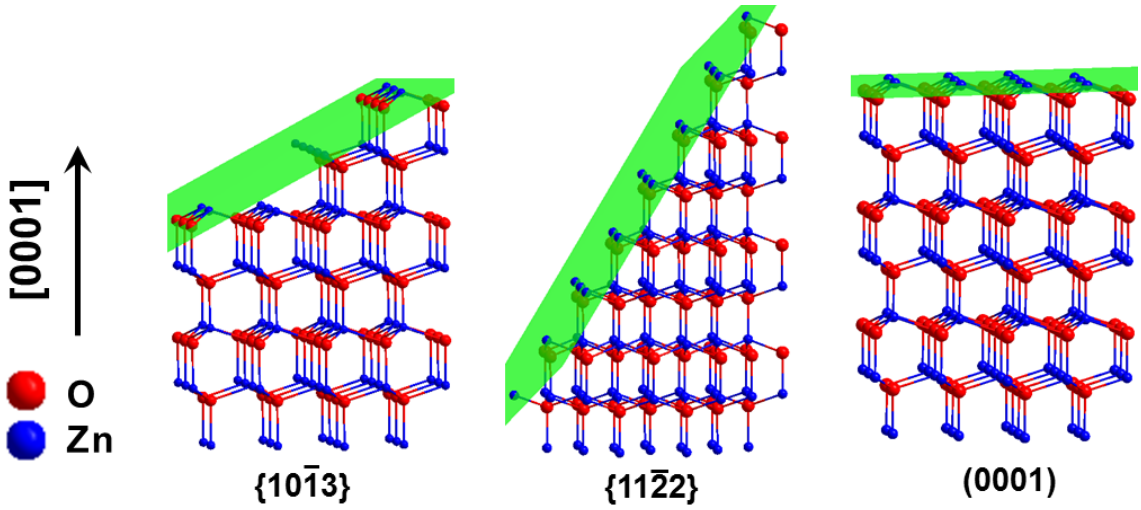

Figure S5. Ball structure models of the facet $\{10\bar{1}3\}$, $\{11\bar{2}2\}$ and (0001).

S7. Calculation about the supersaturation and the growth energy barriers

S7.1. Conversion of the deposition locations to the supersaturation

Since the facet evolution region is very narrow (~1 cm) and at the high temperature region, where the temperature change could be neglected (Figure S2). It is assumed that the temperature is constant in this region (1665 K). Therefore, the supersaturation is not affected by the temperature. Since considerable amount of deposition occurred in this region, the zinc vapor concentration decreases due to the consumption of deposition, which is considered as the solo parameter that changes the supersaturation (decreases along the downstream direction).

According to our previous calculation results, the deposition location could be related to the supersaturation through the equation S1 below:

$$\sigma = \frac{c_0 RT - P_e}{P_e} - \frac{4R_{con} \cdot RT}{P_e \cdot D \cdot r} \cdot x \qquad \text{(S1)}$$

where σ is the supersaturation, c_0 is the initial vapor concentration, R is gas constant, T is the deposition temperature, P_e is the vapor pressure in equilibrium, R_{con} is the deposition rate, D is the internal diameter of the furnace tube, r is the flow rate of the carrier gas, and x is the deposition location. With this equation, we divided the facet evolution region into a series of finite small areas and in each finite small area, the supersaturation is constant. The supersaturation is successively calculated based on the previous one. Thus, we could estimate the supersaturation for each interested NW.

The converted results from deposition locations to the supersaturation are listed below:

Facet evolutions	Distance to the chamber center (cm)	supersaturation
(0001)&{$10\bar{1}3$}	17.693	0.0366
(0001)&{$10\bar{1}3$}	17.823	0.0316
(0001)&{$10\bar{1}3$}	17.879	0.0267
(0001)&{$10\bar{1}3$}	17.915	0.0223
(0001)&{$10\bar{1}3$}	17.999	0.0180
{$10\bar{1}3$}&{$11\bar{2}2$}	18.101	0.0145
{$10\bar{1}3$}&{$11\bar{2}2$}	18.265	0.0104
{$10\bar{1}3$}&{$11\bar{2}2$}	18.301	0.0074

$\{11\bar{2}2\}\&(0001)$	18.304	0.0052
$\{11\bar{2}2\}\&(0001)$	18.398	0.0035
$\{11\bar{2}2\}\&(0001)$	18.490	0.00344
$\{11\bar{2}2\}\&(0001)$	18.554	0.003366
$\{11\bar{2}2\}\&(0001)$	18.570	0.003349
$\{11\bar{2}2\}\&(0001)$	18.710	0.003197

S7.2. Calculation of the growth energy barrier differences.

The growth rate ratio could be expressed as follows:

$$\frac{v_1}{v_2} = \exp(-\frac{\Delta E}{kT}) \qquad \text{(S2)}$$

where v_1, v_2 are the growth rate of facet 1 and facet 2, respectively, ΔE is the difference of the growth energy barrier between facet 1 and facet 2, k is Boltzmann constant and T is the deposition temperature. Based on Eq. S2, the growth rate ratio calculated from the area ratio of facet 1 and facet 2, and the measured deposition temperature, ΔE could be obtained for each interested NW.